# A Microfabricated Platform to Measure and Manipulate the Mechanics of Engineered Cardiac Microtissues

Thomas Boudou, Ph.D.,[1] Wesley R. Legant,[1] Anbin Mu,[2] Michael A. Borochin,[1] Nimalan Thavandiran,[3]
Milica Radisic, Ph.D.,[3] Peter W. Zandstra, Ph.D.,[3] Jonathan A. Epstein, M.D.,[2,4]
Kenneth B. Margulies, M.D.,[2] and Christopher S. Chen, M.D., Ph.D.[1]

Engineered myocardial tissues can be used to elucidate fundamental features of myocardial biology, develop organotypic *in vitro* model systems, and as engineered tissue constructs for replacing damaged heart tissue *in vivo*. However, a key limitation is an inability to test the wide range of parameters (cell source, mechanical, soluble and electrical stimuli) that might impact the engineered tissue in a high-throughput manner and in an environment that mimics native heart tissue. Here we used microelectromechanical systems technology to generate arrays of cardiac microtissues (CMTs) embedded within three-dimensional micropatterned matrices. Microcantilevers simultaneously constrain CMT contraction and report forces generated by the CMTs in real time. We demonstrate the ability to routinely produce ∼200 CMTs per million cardiac cells (<1 neonatal rat heart) whose spontaneous contraction frequency, duration, and forces can be tracked. Independently varying the mechanical stiffness of the cantilevers and collagen matrix revealed that both the dynamic force of cardiac contraction as well as the basal static tension within the CMT increased with boundary or matrix rigidity. Cell alignment is, however, reduced within a stiff collagen matrix; therefore, despite producing higher force, CMTs constructed from higher density collagen have a lower cross-sectional stress than those constructed from lower density collagen. We also study the effect of electrical stimulation on cell alignment and force generation within CMTs and we show that the combination of electrical stimulation and auxotonic load strongly improves both the structure and the function of the CMTs. Finally, we demonstrate the suitability of our technique for high-throughput monitoring of drug-induced changes in spontaneous frequency or contractility in CMTs as well as high-speed imaging of calcium dynamics using fluorescent dyes. Together, these results highlight the potential for this approach to quantitatively demonstrate the impact of physical parameters on the maturation, structure, and function of cardiac tissue and open the possibility to use high-throughput, low volume screening for studies on engineered myocardium.

## Introduction

Cardiac tissue engineering is a promising pathway to address the problem of ischemic heart disease, the leading cause of death in developed countries.[1] Engineered myocardial tissues can be used to study fundamental myocardial biology, as well as to generate *in vitro* models of human cardiac tissue. Such models may find use in the development of clinical therapies or for the examination of the functional effects of patient-specific mutations. Furthermore, several techniques have been developed to generate cardiac tissues *in vitro*, with the goal of replacing damaged heart tissue *in vivo*.[2] The majority of such approaches have focused on pre-seeding centimeter-scale scaffolds with a variety of cell sources,[3–7] allowing the cells to mature under appropriate soluble and mechanical conditions *in vitro* and then surgically attaching the cell-based cardiac grafts to the myocardium.[8–11] The use of these techniques, combined with recently developed methods for generating cardiomyocytes from human embryonic stem cells[12–14] and induced pluripotent stem cells,[15–17] is an exciting avenue for the treatment of damaged heart tissue.[18,19]

In a pioneering study, Zimmermann and colleagues demonstrated functional improvements upon implantation of engineered heart tissue in rat with left descending coronary artery ligation. However, because current engraftments

---

[1]Department of Bioengineering, University of Pennsylvania, Philadelphia, Pennsylvania.
[2]Cardiovascular Institute, University of Pennsylvania, Philadelphia, Pennsylvania.
[3]Institute of Biomaterials and Biomedical Engineering, University of Toronto, Toronto, Canada.
[4]Department of Cell and Developmental Biology, University of Pennsylvania, Philadelphia, Pennsylvania.

have shown only modest improvements in cardiac function, there is a clear need to understand what conditions could improve the functional performance of engineered cardiac tissue.[10] Recently, several studies demonstrated that the structural and functional properties of engineered myocardium *in vitro* were improved by the use of electrical stimulation,[20–22] the application of cyclic mechanical stretch,[23,24] or the incorporation of noncardiac myocyte stromal cells such as cardiac fibroblasts and endothelial cells.[25,26] A key limitation to the advancement of cardiac tissue engineering is an inability to test each of these parameters (cell source, mechanical, soluble and electrical stimuli) in a high-throughput and combinatorial manner. Furthermore, no method currently exists that can measure both fine-scale cytoskeletal and extracellular architecture as well as cardiac contractility, the ultimate functional output of the myocardium. Due to their size, centimeter-scale constructs are too expensive to generate in a high-throughput manner and require histological sectioning to visualize cellular and extracellular architecture. In contrast, traditional two-dimensional (2D) high-throughput platforms are well established, but fail to recapitulate the mechanical and structural environment of native heart tissue.

Here we present an approach to generate cardiac microtissues (CMTs), microscale constructs of cardiac cells embedded within collagen/fibrin three-dimensional (3D) matrices, in our previously developed microfabricated tissue gauges (µTUGs).[27] These µTUGs incorporate microelectromechanical systems (MEMS) cantilevers, which simultaneously constrain and report forces generated by the CMTs in real time. We previously applied these devices to the study of fibroblast-induced collagen reorganization.[27] In that study, we also reported that plating cardiomyocytes into the µTUGs resulted in an occasional, very low frequency CMT. Here, we report the results of optimizations of this tool for high-yield CMT formation. We demonstrate the ability to routinely produce hundreds of functional CMTs from readily available cardiac cells and we monitor their spontaneous contraction frequency, duration, and forces. We examine the influence of the mechanical stiffness of the cantilevers and the extracellular matrix on the remodeling and contractility of CMTs. Moreover, we modify the initial µTUGs by introducing carbon electrodes to study the effect of electrical stimulation on cell alignment and force generation within CMTs. Finally, we demonstrate the potential of our technique for high-throughput, low volume drug screening by analyzing the dose-response effect of chronotropic and inotropic drugs on CMTs. Together, these results highlight a unique approach to examine the effects of various stimuli such as mechanical preload, matrix stiffness, electrical stimulation, or soluble factors on the structural and functional properties of engineered CMTs.

## Materials and Methods

### Cell culture and reagents

Cardiomyocytes were isolated from 0 to 1-day neonatal Sprague Dawley rat pups by a Trypsin digestion protocol as previously described.[28] The resulting cell population was immediately subjected to CMT generation. CMTs were cultured in high-glucose DMEM (Mediatech, Inc.) containing 10% horse serum (Invitrogen), 2% chick embryo extract (Charles River Laboratories International, Inc.), 4 mM L-glutamine, 1 mM sodium pyruvate, 100 units/mL penicillin, and 100 mg/mL streptomycin (all from Invitrogen). Cell culture medium was changed every day. Stock solution of Isoproterenol (Sigma-Aldrich) of 10 mM was made in MilliQ water and stock solution of Digoxin (GlaxoSmithKline) of 10 mM was made in DMSO. Calcium staining was obtained by incubating CMTs for 1 h with the acetoxymethyl ester of fluo-3 [fluo-3/(AM); Invitrogen] as a fluorescent dye at 2 µM in phosphate-buffered saline (PBS) with 0.02% of Pluronic F127 (BASF).

### Device fabrication

SU-8 masters were fabricated following a modified version of the technique described previously.[27] Briefly, layers of SU-8 photoresist (Microchem) were patterned onto silicon wafers by successive spin coat, alignment, exposure, and bake steps. Polydimethylsiloxane (PDMS, Sylgard 184, Dow-Corning) µTUG substrates were molded from the SU-8 masters as described previously[29] with an additional step of embedding fluorescent microbeads (Fluoresbrite 17147; Polysciences, Inc.) into the cantilevers to accommodate computerized cantilever deflection tracking. PDMS stamps were submerged in ethanol and treated in an ultrasonic pen cleaner (Model 600; Rotex Co.) to displace air trapped in the inverted pattern. After 5 min, the stamps were transferred into the wells of a six-well plate and 10 mL of ethanol and fluorescent bead solution (3000:1) was added to each well. The six-well plates containing stamps were then centrifuged for 1 min at 1000 rpm to settle the fluorescent beads into the pattern on the stamps. The ethanol was then allowed to evaporate overnight at room temperature, leaving the beads behind covering the entire patterned surface. PDMS molds were then cast onto the stamps to produce the final µTUG substrates. As a result, the fluorescent beads covering the stamp were embedded in the surface of the substrates.

### Calculation of cantilever spring constant

Cantilever spring constants were calculated utilizing a capacitive MEMS force sensor mounted on a micromanipulator as described previously.[30] Images of the sensor tip and cantilever head were acquired during each test using an Olympus FV1000 confocal microscope with an air-immersion 0.4 NA 10× objective. To account for local deformation of the PDMS material around the sensor, the spring constant of the MEMS sensor was calibrated against the side of the PDMS well, which can be viewed as an elastic half space of the same material modulus as the PDMS cantilevers and was found to be 104 ± 1.9 nN/µm. This value was then used for the subsequent measurements of the force required for cantilever bending. For each measurement, the sensor tip was placed 20 µm below the top of the post and the probe translated laterally against the outer edge of the cantilever using a custom-written Lab View (National Instruments) script. The probe base was displaced ∼150 µm for each measurement. The displacement of the probe tip (and thus of the cantilever head) was calculated from the spring constant measured previously and the reported sensor force and was verified visually during the deformation. Five cantilevers were measured across a substrate and measurements were repeated for three different substrates of each condition.

Cantilevers were found to have linear responses up to ~30 μm of deformation, beyond which the response became nonlinear. As the cantilever deformations observed in this paper were all below 30 μm, this section was fit using a linear fit. The spring constant of the rigid and flexible cantilevers across a substrate was found to be $0.45 \pm 0.10$ μN/μm and $0.20 \pm 0.03$ μN/μm, respectively.

### Microtissue seeding

Before cell seeding, the PDMS templates were sterilized in 70% ethanol followed by UV irradiation for 15 min and treated with 0.2% Pluronic F127 for 60 min to reduce cell adhesion. A reconstitution mixture, consisting of 1 mg/mL or 2.5 mg/mL liquid neutralized collagen I from rat tail (BD Biosciences) and 0.5 mg/mL fibrinogen from bovine plasma (Sigma-Aldrich), was then added to the surface of the substrates on ice and templates were degassed under vacuum to remove bubbles in the liquid. A cooled suspension of half a million cells within reconstitution mixture was then added to the substrate and the entire assembly was centrifuged to drive the cells into the micropatterned wells, resulting in approximately 500 cells per well. Excess collagen/fibrinogen and cells were removed by de-wetting the surface of the substrate before incubating at 37°C to induce collagen polymerization. The appropriate media were then added to each substrate. By using a live/dead cell viability assay (Invitrogen), we estimated cell viability over time. The average ratio of living cells after seeding in the μTUGs is of $64\% \pm 9\%$, statistically similar to the viability right after isolation ($69\% \pm 11\%$), and slowly decreases to $46\% \pm 13\%$ after 7 days of culture.

### Force quantification

For quantifying microtissue forces, brightfield and fluorescence images were taken at 20 Hz within each template, using a Photometrics Evolve EMCCD camera (Photometrics), and an A-Plan 10× objective on a Nikon Eclipse Ti (Nikon Instruments, Inc.) equipped with a live cell incubator. Only tissues that were uniformly anchored to the tips of the cantilevers were included in the analysis. The displacement of fluorescent microbeads at the top of the cantilevers was then tracked with using the SpotTracker plug-in[31] in ImageJ (National Institutes of Health).

### Electrical stimulation

Electrical stimulation was started 3 days after cell seeding, by placing two carbon electrodes (1/4 in diameter; Ladd Research Industries) on the sides of the samples (separated by 2 cm), connected through platinum wires to a stimulator as described previously.[21] Voltage threshold (VT) is the minimum voltage at which the CMTs are observed to beat synchronously under electrical field stimulation at 1 Hz using 1 ms square biphasic pulses. Maximum capture rate (MCR) is defined as the maximum pacing frequency for synchronous contractions at ~20% over VT. Continuous stimulation was achieved by using biphasic square pulses of 1 ms at 6 V/cm and 0.2 Hz.[22]

### Immunofluorescence and image analysis

Microtissues were fixed with 4% paraformaldehyde in PBS, permeabilized with 0.2% Triton X-100 in PBS, incubated with antibodies against troponin T (Thermo Scientific), and detected with fluorophore-conjugated, isotype-specific, anti-IgG antibodies and counterstained with DAPI (Invitrogen). Alignment was quantified from DAPI images by fitting ellipses with ImageJ. Nuclei were considered aligned when the angle between their long axis and the x-axis (the axis joining the two cantilevers) was less than 20°. Cross-sectional areas were estimated from z-stack images obtained with a 40× water-immersion objective attached to a laser scanning microscope Zeiss LSM 510 (Carl Zeiss, Inc.).

### Statistical comparisons

Statistical comparisons were based on an analysis of variance for pairwise comparisons ($p < 0.05$ was considered significant).

## Results

### Generation of CMTs

To generate microscale constructs of cardiac cells within collagen/fibrin 3D matrices, we microfabricated arrays of wells within a PDMS mold. The mold was immersed in a suspension of cells and reconstitution mixture (liquid neutralized collagen I and fibrinogen) and the entire assembly was centrifuged to drive the cells into the micropatterned wells. Excess collagen/fibrinogen and cells were removed and the remaining constructs were polymerized. Over time of cultivation, the cells spread inside the matrix, form cell–cell contacts, and spontaneously compact the matrix over several days (Fig. 1A). Two T-shaped cantilevers incorporated within each template anchor the contracting matrix, constraining the contraction of the collagen/fibrin matrix to form a linear band that spanned across the top of the pair of cantilevers. This resulted in a large array of CMTs anchored to the tips of the cantilevers per substrate. The spring constant of each cantilever could be controlled by altering the ratio between PDMS and curing agent. We used linear bending theory and experimental measurements to report the load-displacement relationship for two different ratios PDMS/curing agent, leading to measured spring constants of 0.45 and 0.20 μN/μm. These spring constants were then used to link the measured cantilever deflections to the amount of force generated by CMTs (Fig. 1B).

After cell seeding, at day 0, the collagen/fibrin matrix contained evenly distributed, amorphous, round heart cells (Fig. 1A). Over time, cells elongated, aligned along the axis between the cantilevers, and started to beat as single cells at days 1–2 at a spontaneous frequency of $1.1 \pm 0.1$ Hz. Remodeling and compaction of the matrix led to a slower and coherent beating, rhythmically deflecting the posts at $0.5 \pm 0.1$ Hz after day 3 (Fig. 1C), and to a marked reduction of construct size (final diameter 50–70 μm at the thinnest portion of the construct at day 7). The beating frequency is slower than the beat rate of an intact adult rat heart (5–7 Hz)[10] or a neonatal rat heart (4–6 Hz)[32] but close to frequencies measured in centimeter-scale cardiac tissues generated from isolated cardiomyocytes.[5,33] Over time of cultivation, the total contraction duration (contraction and relaxation) appeared to be roughly stable around $0.25 \pm 0.01$ s (Fig. 1D), similar to contraction durations measured in centimeter-scale cardiac tissues.[23]
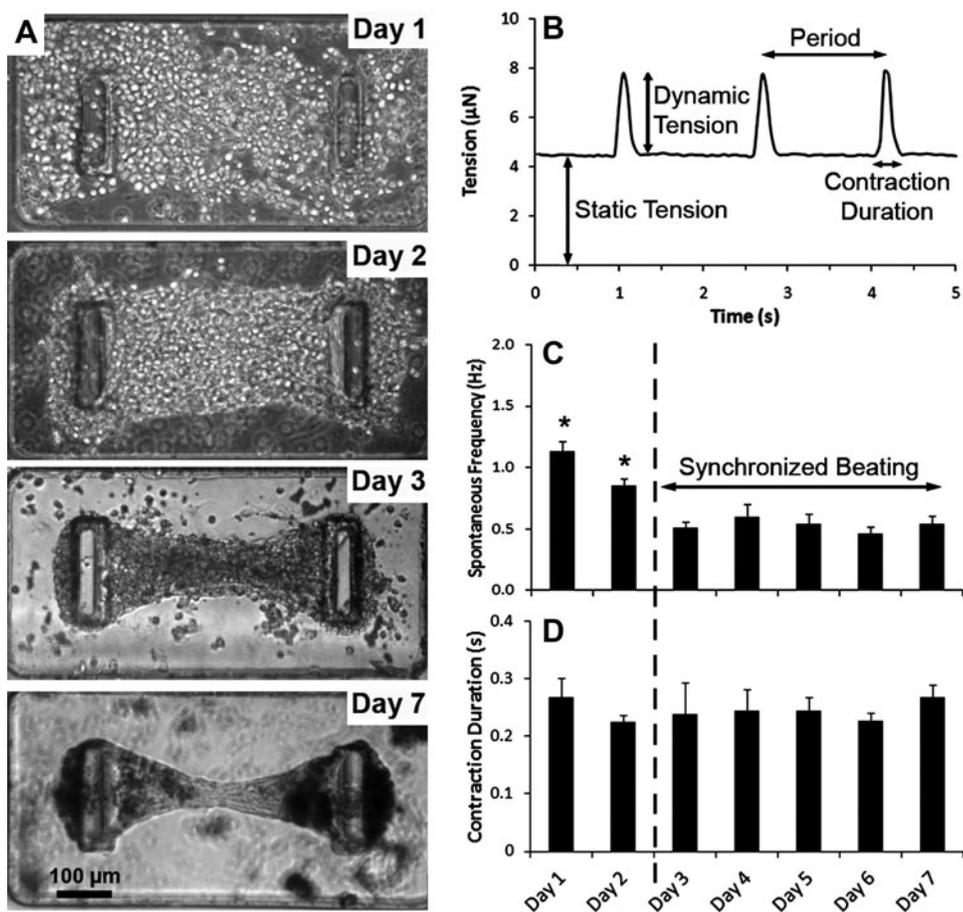
**FIG. 1.** Temporal evolution of CMTs constructed in 0.5 mg/mL fibrin and 1.0 mg/mL collagen gels and tethered to rigid ($k = 0.45 \mu N/\mu m$) cantilevers. **(A)** Representative images depicting the time course of a contracting CMT. **(B)** Representative recording of the tension as a function of the time of a CMT on day 5. **(C)** Temporal evolution of the spontaneous beating frequency and **(D)** of the contraction duration of beating (contraction and relaxation). Data are the average of 15 CMTs ± SEM. *$p < 0.01$. CMT, cardiac microtissue.

*Influence of the stiffness of the environment*

Interestingly, the spring constant of the cantilevers impacted both the dynamic and the static tension generated by cells. The dynamic tension is defined as the force exerted during contractile beatings of CMTs and is only due to cardiomyocytes whereas the static tension is due to the baseline tonic traction of all the cells that leads to the compaction of the matrix (Fig. 1B). Indeed, by staining for troponin-T, we determined that our native cell isolate contained 58% ± 3% cardiac myocytes and it has been shown that native myocardium consists of multiple cell types, including cardiomyocytes and up to 50% of nonmyocytes (fibroblasts and endothelial cells), which are actively involved in crosstalk.[34] Beating contractions of CMTs tethered to flexible cantilevers ($k = 0.20 \mu N/\mu m$) at day 5 generated 2.39 ± 0.24 μN whereas CMTs tethered to more rigid cantilevers ($k = 0.45 \mu N/\mu m$) generated twofold more force (Fig. 2A). The static tension was also lower between flexible cantilevers than CMTs between rigid cantilevers but the relative impact was less substantial (6.03 ± 0.36 vs. 8.25 ± 0.61 μN, respectively). The lower contractility of CMTs tethered to flexible cantilevers appeared to result in decreased compaction of the collagen/fibrin matrix by the cells (Fig. 2B), resulting in 3.4-fold lower dynamic cross-sectional stress (i.e., tension normalized by the cross-sectional area) and twofold lower static cross-sectional stress at day 5 (Fig. 2C, D). These cross-sectional stresses are lower than those measured in intact heart muscle[35] or in centimeter-scale engineered tissues.[5] This may be

due to low number of cardiac cells in our constructs and their short maturation time (only 7 days).

In addition to the cantilever stiffness, we examined the influence of the bulk modulus of the collagen/fibrin matrix on the contractility of CMTs. We observed that the static tensions increased when the collagen density was increased from 1.0 to 2.5 mg/mL (Fig. 3A). However, this higher static tension in CMTs constructed from 2.5 mg/mL collagen was not sufficient to overcome the increased rigidity of the denser collagen matrix (Fig. 3B), thus leading to less matrix remodeling and lower values of both dynamic and static stresses (Fig. 3C, D). These results highlight an interesting difference in the relative feedback of boundary rigidity versus matrix stiffness on CMT contractions. Whereas both stiff cantilevers and stiff matrix result in higher cell tension, the cell alignment stays limited by the mechanical resistance of the stiff matrix, leading to lower cross-sectional stress.

*Electrical stimulation and calcium signaling*

By modifying the μTUGs, we were able to insert two parallel carbon electrodes on both sides of the arrays and thus stimulate simultaneously arrays of CMTs (Fig. 4A and Supplementary Movie S1; Supplementary Data are available online at www.liebertonline.com/tea). Electrical stimulation (biphasic pulses, 6 V/cm, 0.2 Hz, 1 ms) was initiated 3 days after cell seeding and maintained until day 7. We examined the functionality of CMTs every day by three parameters:

**FIG. 2.** Influence of the pillar stiffness on dynamic and static contractility of CMTs constructed in 0.5 mg/mL fibrin and 1.0 mg/mL collagen gels. **(A)** Average tension, **(B)** cross-sectional area, and **(C)** cross-sectional stress for CMTs tethered to flexible ($k=0.20\,\mu N/\mu m$) or rigid ($k=0.45\,\mu N/\mu m$) cantilevers at day 5. Data are the average of 15 CMTs $\pm$ SEM. **(D)** Corresponding phase-contrast images. $*p<0.01$; $**p<0.01$.
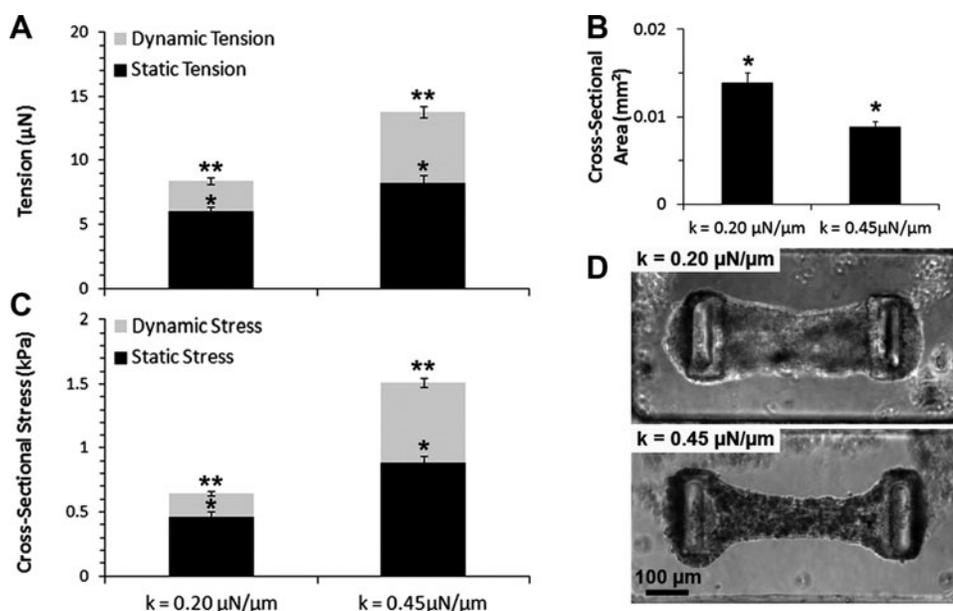
voltage threshold (VT), maximum capture rate (MCR), and cross-sectional stress. VT and MCR were found to be stable over days and similar for nonstimulated (VT = $3.6\pm0.1$ V/cm and MCR = $7.0\pm0.3$ Hz) and stimulated CMTs (VT = $3.5\pm0.1$ V/cm and MCR = $7.2\pm0.3$ Hz) (Fig. 4B, C). The obtained VT and MCR values are slightly higher than those measured previously, which maybe explained by the use of nonenriched cardiac cells in our study.[20,21] Interestingly, continuous electrical stimulation tends to accelerate the generation of higher dynamic contraction stress ($587\pm61$ Pa vs. $419\pm69$ Pa at day 4, after 24 h of stimulation) and to strongly increase the generated static stress (almost twofold higher at day 7 after 4 days of stimulation) (Fig. 4D). We quantified the cell alignment by staining cell nuclei before measuring their orientation (Fig. 5A–E). About 75% of the nuclei are aligned along the CMT long axis at day 4 in the case of stimulated

CMTS, after only 24 h of stimulation, whereas nonstimulated CMTs reach this level of organization after 6 days of culture (Fig. 5E). These data support previous results suggesting that electrical stimulation provides cardiomyocytes with maturation signals.

In addition, we examined whether electrical signals conduct across the engineered tissues by exposing constructs to a fluorescence-based calcium indicator and taking fluorescence images at 30 Hz. We observed spontaneous, periodic calcium release in cells within the CMTs, but most notably, we observed synchronized calcium release across the entire microtissue (Fig. 5F and Supplementary Movie S2). We were able to measure both the fluorescence level within the tissue and the displacement of the pillars. Examining time traces of calcium release and tension exerted by the tissue, the two profiles have a similar shape, with the measured tension



**FIG. 3.** Influence of the matrix composition on dynamic and static contractility of CMTs tethered to rigid ($k=0.45\,\mu N/\mu m$) cantilevers. **(A)** Average tension, **(B)** cross-sectional area, and **(C)** cross-sectional stress for CMTs constructed from 0.5 mg/mL fibrin and 1.0 mg/mL or 2.5 mg/mL collagen gels at day 5. Data are the average of 15 CMTs $\pm$ SEM. **(D)** Corresponding phase-contrast images. $*p<0.01$, $**p<0.01$.
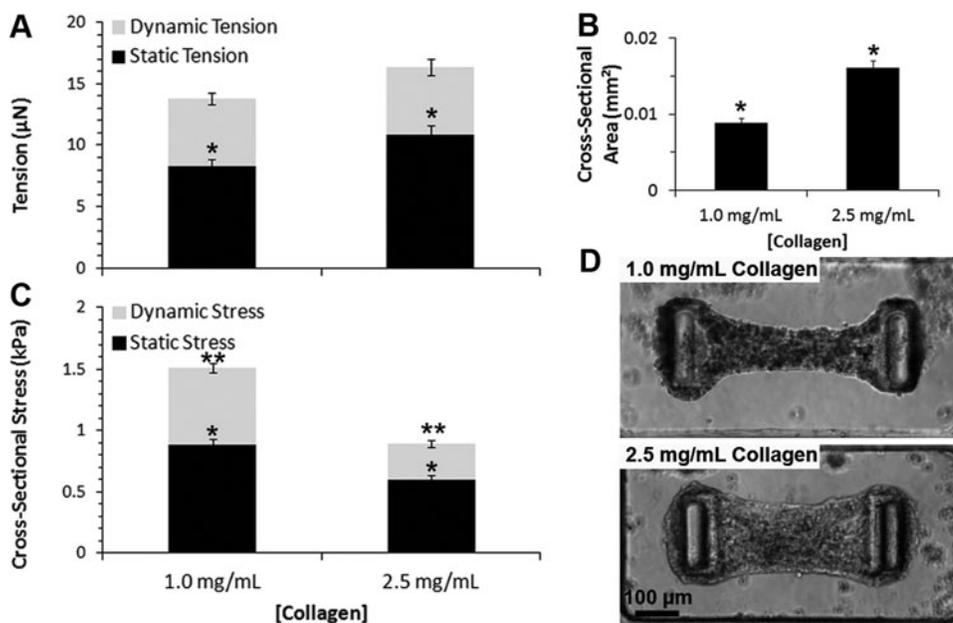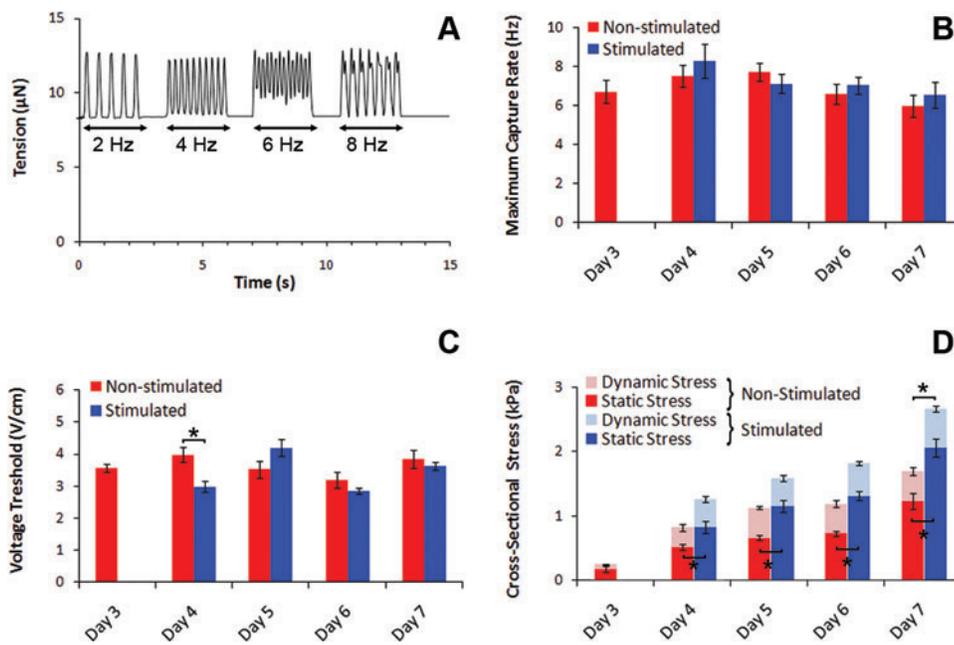
FIG. 4. Functional properties over days of non-stimulated and electrically stimulated CMTs constructed in 0.5 mg/mL fibrin and 1.0 mg/mL collagen gels and tethered to rigid ($k = 0.45\,\mu N/\mu m$) cantilevers. (A) Representative recording of the tension in function of the time and the pacing rate of a non-stimulated CMT on day 5. (B) Maximum capture rate. (C) Voltage threshold. (D) Static and dynamic cross-sectional stress. Data from (B–D) are the average of 10 CMTs ± SEM. *$p < 0.01$. Color images available online at www.liebertonline.com/tea

slightly phase-delayed compared to the calcium release (Fig. 5G). This synchronized calcium release was observed with coherent beating and the maturation of the CMTs after ~3 days of culture, and was associated with the development of sarcomeric structures (Fig. 5A–E). Immunostaining of CMTs initially showed almost random network of troponin-T–positive cardiac myocytes at day 3 (Fig. 5A, B) that longitudinally aligned and elongated, with well-developed parallel cross-striation pattern, consistent with sarcomeric structures, after 7 days of culture (Fig. 5C, D).

### Drug testing

To demonstrate the potential of these CMTs for studying responses to pharmacologic agents, we examined whether CMTs responded appropriately to two well-known cardiac compounds, isoproterenol and digoxin. To study the dose response of the CMTs to these compounds, we varied their concentrations from 1 nM to 10 μM and measured the dynamic stress and the spontaneous frequency of CMTs after 1 h (Fig. 6). Isoproterenol is a β-adrenergic agonist with a well-known positive chronotropic effect[36,37] whereas digoxin is a cardiac glycoside that inhibits $Na^+/K^+$-ATPase (sodium pump),[38,39] activates sarcoplasmic reticulum $Ca^{2+}$-release channels,[40] and induces positive inotropic effects.[40,41] Isoproterenol had no effect at 1 nM, a slight positive inotropic action (increase in contractility) at 10 and 100 nM, and a slight negative inotropic effect (decrease in contractility) at 1 and 10 μM. In contrast, isoproterenol had a strong positive chronotropic action at 1 and 10 μM, doubling the spontaneous frequency at 1 μM and tripling it at 10 μM. Digoxin led to a positive inotropic response between 1 nM and 1 μM, with a maximal stress increase of 22% ± 4% at 1 μM. At 10 μM, digoxin appears to be cardiotoxic with almost no inotropic effect but a strong negative chronotropic effect with a spontaneous frequency dropping under 0.04 ± 0.01 Hz. These results demonstrate that the mechanical response of CMTs could be used to understand the functional consequences of pharmacologic agents.

## Discussion

The potential uses of engineered myocardial tissues are both diverse and powerful. Recent studies reported that the key modulators of engineered myocardium are not only the cell composition, differentiation, and orientation,[3,23,34] but also the embedding matrix composition[5,42] and the external stimuli such as cyclic stretching or electrical stimulation.[21,23,43,44] In response to these inputs, the most important outputs of engineered heart tissues are force generation and contraction characteristics. Unfortunately, few platforms are available to measure force, a limitation starkly highlighted by the fact that current protocols for deriving cardiomyocytes from stem cells and induced pluripotent stem cells rely on staining for cardiac myocyte markers,[12–17] rather than on force generation. Here we try to bridge this gap by providing a simple approach to generate micrometer-scale cardiac tissues from neonatal rat heart cells and to measure the forces and mechanical stresses they exert during matrix remodeling and twitch contractions.

Our technique allows the routine preparation of ~200 CMTs per million cardiac cells (<1 neonatal rat heart) that are well-suited for examining how biomechanical cues influence the structure and function of engineered myocardial tissue. Within days of cultivation, we observed the compaction of the matrix by the cells, which bends the posts toward each other. The reactive force of the posts imposes a mechanical preload on each construct. Previously, it has been shown that performing contractile work against elastic boundaries (also called "auxotonic" load), similar to the beating heart against the elastic resistance of the circulation, improves cardiac tissue development.[10] Elastic boundaries thus enhance the development of the sarcoplasmic reticulum in cardiomyocytes, resulting in higher cell tension,[5,10] as confirmed by the large forces generated by CMTs tethered to our cantilevers. This high cell tension leads to a strongly compacted extracellular matrix, an increased alignment of the cells, and a better development of the sarcomeric
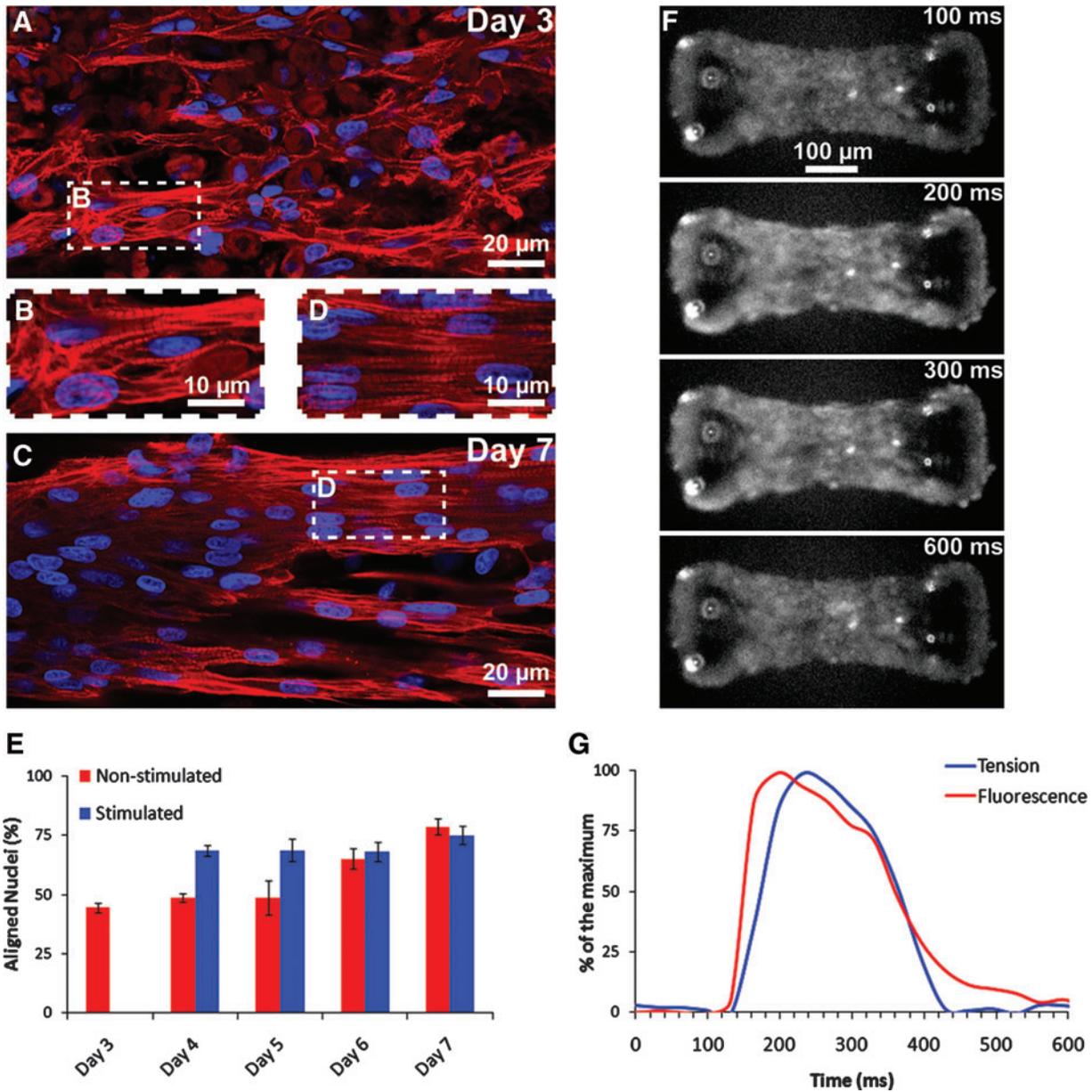
**FIG. 5.** Structural properties and calcium signaling of CMTs constructed in 0.5 mg/mL fibrin and 1.0 mg/mL collagen gels and tethered to rigid ($k = 0.45\,\mu N/\mu m$) cantilevers. **(A, B)** Immunostaining of troponin-T (red) and nuclei (blue) in a representative CMT at day 3 and **(C, D)** at day 7. **(E)** Percentage of aligned nuclei (angle < 20°). **(F)** Time series fluorescence images of a CMT after incubation with calcium indicator fluo-3. **(G)** Representative simultaneous recording of the fluorescence of the calcium indicator and the tension exerted by a CMT. Data from **(E)** are the average of 6 CMTs ± SEM. Color images available online at www.liebertonline.com/tea

structures, resulting in a higher cross-sectional stress generated by the tissue. Previous studies using 2D substrates have demonstrated that substrate stiffness can regulate cardiac function. Indeed, following a myocardial infarction, beating cardiomyocytes are replaced by a fibrotic scar ($E \approx 35$–$70\,kPa$) that is several-fold stiffer than normal myocardium ($E \approx 5$–$15\,kPa$)[45] and it has been shown recently that spontaneous contractions,[42] cytoskeletal organization,[46] or differentiation[47] of cardiomyocytes were strongly influenced by such change in stiffness. Here we demonstrated that the density of 3D collagen/fibrin matrix can feedback to increase contractile forces of cardiac cells embedded within it.

Simultaneously, the matrix composition has a direct impact on the ability of the cells to reorganize within the matrix and to remodel it. We thus found that a denser matrix is less compacted by the cells, resulting in a poor alignment of the cells and a lower efficiency of the cardiac tissue, characterized by the generated cross-sectional stress. By inserting carbon electrodes within the μTUGs, we showed that electrical stimulation induces a better compaction of the matrix by the cells and a faster alignment of the cells, improving the cell coupling. By forcing the CMTs to beat periodically over days, electrical stimulation may also increase the positive effect of the auxotonic load due to the stiff cantilevers and
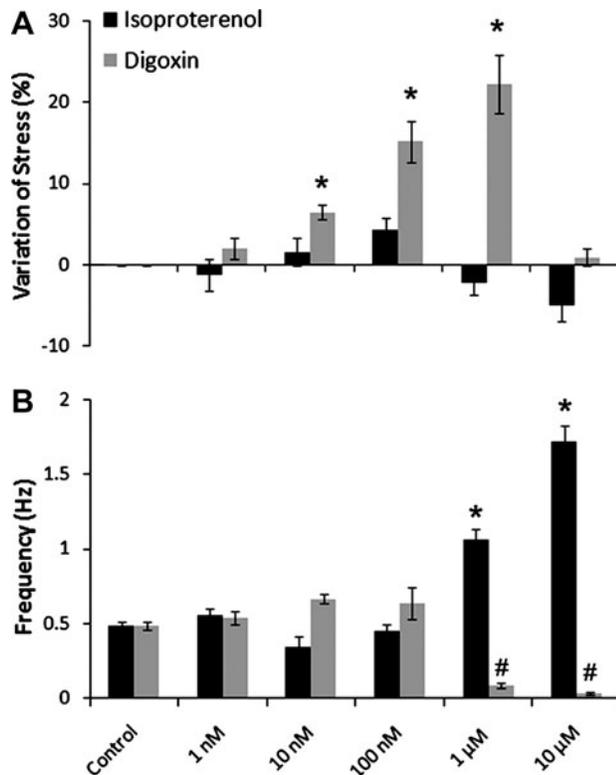
**FIG. 6.** Effects of isoproterenol and digoxin on CMT functionality. **(A)** Variation of the dynamic cross-sectional stress compared with the control and **(B)** of the beating frequency in function of the drug concentration. Data are the average of 10 CMTs ± SEM. $*p < 0.01$; $\#p < 0.01$.

leads to higher cross-sectional stress. The combination of electrical stimulation and auxotonic load thus appears to strongly improve both the structure and the function of the CMTs while demonstrating the fundamental importance of biomechanical cues as regulators of myocardial structure and function.

We also demonstrated that our microtissue assay is suitable for high-throughput monitoring of drug-induced changes in spontaneous frequency or contractility in CMTs. The micrometer scale of the CMTs allows for rapid penetration of soluble effectors into the constructs. Both isoproterenol and digoxin produced reproducible, dose-dependent effects on microtissue contractility and beating frequency. Because it has minimal effects on beating frequency, the dose-response studies with the $Na^+/K^+$-ATPase inhibitor digoxin demonstrated clear thresholds for both inotropic and toxic effects, with values that are typical for this compound.[41] In contrast, the β-adrenergic agonist isoproterenol demonstrated dose-dependent chronotropic responses, but rather blunted inotropy compared with findings typical of native rat myocardium.[48] This discrepancy in contractile responses could be due to immature β-adrenergic signaling in neonatal cardiomyocytes at day 7 or a confounding negative effect of increased beating frequency on contractility since rat myocardium is known to have a frequency-dependent force production.[49–51]

In conclusion, the overall similarity of structural and functional characteristics between CMTs and *in vivo* heart muscle is promising and our novel method for CMT generation opens the potential to high-throughput, low volume screening applications. Moreover, the model's ability to quantitatively demonstrate the impact of physical parameters on the maturation, structure, and function of cardiac tissue provides unique opportunities to elucidate mechanisms of load-dependent myocardial remodeling in stable, 3D, working muscle preparations. Most importantly, the model provides reproducible contractile phenotyping that is virtually absent in 2D culture models. These same attributes will likely provide valuable opportunities to elucidate how biomechanical, electrical, biochemical, and genetic/epigenetic cues modulate the differentiation and maturation of stem cells. Thus, combining stem cell differentiation and microtissue engineering could pave the way to the production of high-quality functional myocardium from stem cells, opening an exciting avenue for the treatment of damaged heart tissue.

## Disclosure Statement

No competing financial interests exist.

## References

1. Mathers, C.D., Bernard, C., Iburg, K.M., Inoue, M., Ma Fat, D., Shibuya, K., Stein, C., Tomijima, N., and Xu, H. Global Burden of Disease: Data Sources, Methods and Results. World Health Organization, Geneva, Switzerland, 2008.
2. Eschenhagen, T., and Zimmermann, W.H. Engineering myocardial tissue. Circ Res **97,** 1220, 2005.
3. Carrier, R.L., Papadaki, M., Rupnick, M., Schoen, F.J., Bursac, N., Langer, R., Freed, L.E., and Vunjak-Novakovic, G. Cardiac tissue engineering: cell seeding, cultivation parameters, and tissue construct characterization. Biotechnol Bioeng **64,** 580, 1999.
4. van Luyn, M.J.A., Tio, R.A., Gallego y van Seijen, X.J., Plantinga, J.A., de Leij, L.F.M.H., DeJongste, M.J.L., and van Wachem, P.B. Cardiac tissue engineering: characteristics of in unison contracting two- and three-dimensional neonatal rat ventricle cell (co)-cultures. Biomaterials **23,** 4793, 2002.
5. Hansen, A., Eder, A., Bonstrup, M., Flato, M., Mewe, M., Schaaf, S., Aksehirlioglu, B., Schworer, A., Uebeler, J., and Eschenhagen, T. Development of a drug screening platform based on engineered heart. Tissue Circ Res **107,** 35, 2010.
6. Kofidis, T., Akhyari, P., Boublik, J., Theodorou, P., Martin, U., Ruhparwar, A., Fischer, S., Eschenhagen, T., Kubis, H.P., Kraft, T., Leyh, R., and Haverich, A. *In vitro* engineering of heart muscle: artificial myocardial tissue. J Thorac Cardiovasc Surg **124,** 63, 2002.

7. Radisic, M., Park, H., Gerecht, S., Cannizzaro, C., Langer, R., and Vunjak-Novakovic, G. Biomimetic approach to cardiac tissue engineering. Philos Trans R Soc B **362,** 1357, 2007.

8. Li, R.-K., Jia, Z.-Q., Weisel, R.D., Mickle, D.A.G., Choi, A., and Yau, T.M. Survival and function of bioengineered cardiac grafts. Circulation **100(19 Suppl),** II63, 1999.

9. Leor, J., Aboulafia-Etzion, S., Dar, A., Shapiro, L., Barbash, I.M., Battler, A., Granot, Y., and Cohen, S. Bioengineered cardiac grafts: a new approach to repair the infarcted myocardium? Circulation **102(19 Suppl 3),** III56, 2000.

10. Zimmermann, W.-H., Melnychenko, I., Wasmeier, G., Didie, M., Naito, H., Nixdorff, U., Hess, A., Budinsky, L., Brune, K., Michaelis, B., Dhein, S., Schwoerer, A., Ehmke, H., and Eschenhagen, T. Engineered heart tissue grafts improve systolic and diastolic function in infarcted rat hearts. Nat Med **12,** 452, 2006.

11. Shimizu, T., Yamato, M., Isoi, Y., Akutsu, T., Setomaru, T., Abe, K., Kikuchi, A., Umezu, M., and Okano, T. Fabrication of pulsatile cardiac tissue grafts using a novel 3-dimensional cell sheet manipulation technique and temperature-responsive cell culture surfaces. Circ Res **90,** e40, 2002.

12. Kehat, I., Kenyagin-Karsenti, D., Snir, M., Segev, H., Amit, M., Gepstein, A., Livne, E., Binah, O., Itskovitz-Eldor, J., and Gepstein, L. Human embryonic stem cells can differentiate into myocytes with structural and functional properties of cardiomyocytes. J Clin Invest **108,** 407, 2001.

13. Niebruegge, S., Bauwens, C.L., Peerani, R., Thavandiran, N., Masse, S., Sevaptisidis, E., Nanthakumar, K., Woodhouse, K., Husain, M., Kumacheva, E., and Zandstra, P.W. Generation of human embryonic stem cell-derived mesoderm and cardiac cells using size-specified aggregates in an oxygen-controlled bioreactor. Biotechnol Bioeng **102,** 493, 2009.

14. Kattman, S.J., Witty, A.D., Gagliardi, M., Dubois, N.C., Niapour, M., Hotta, A., Ellis, J., and Keller, G. Stage-specific optimization of activin/nodal and BMP signaling promotes cardiac differentiation of mouse and human pluripotent stem cell lines. Cell Stem Cell **8,** 228, 2011.

15. Zhang, J., Wilson, G.F., Soerens, A.G., Koonce, C.H., Yu, J., Palecek, S.P., Thomson, J.A., and Kamp, T.J. Functional cardiomyocytes derived from human induced pluripotent stem cells. Circ Res **104,** e30, 2009.

16. Burridge, P.W., Thompson, S., Millrod, M.A., Weinberg, S., Yuan, X., Peters, A., Mahairaki, V., Koliatsos, V.E., Tung, L., and Zambidis, E.T. A universal system for highly efficient cardiac differentiation of human induced pluripotent stem cells that eliminates interline variability. Plos One **6,** e18293, 2011.

17. Ieda, M., Fu, J.-D., Delgado-Olguin, P., Vedantham, V., Hayashi, Y., Bruneau, B.G., and Srivastava, D. Direct reprogramming of fibroblasts into functional cardiomyocytes by defined factors. Cell **142,** 375, 2010.

18. Zimmermann, W.-H. Embryonic and embryonic-like stem cells in heart muscle engineering. J Mol Cell Cardiol **50,** 320, 2011.

19. Sturzu, A.C., and Wu, S.M. Developmental and regenerative biology of multipotent cardiovascular progenitor cells. Circ Res **108,** 353, 2011.

20. Tandon, N., Cannizzaro, C., Chao, P.-H.G., Maidhof, R., Marsano, A., Au, H.T.H., Radisic, M., and Vunjak-Novakovic, G. Electrical stimulation systems for cardiac tissue engineering. Nat Protoc **4,** 155, 2009.

21. Radisic, M., Park, H., Shing, H., Consi, T., Schoen, F.J., Langer, R., Freed, L.E., and Vunjak-Novakovic, G. Functional assembly of engineered myocardium by electrical stimulation of cardiac myocytes cultured on scaffolds. Proc Natl Acad Sci U S A **101,** 18129, 2004.

22. Chiu, L.L.Y., Iyer, R.K., King, J.-P., and Radisic, M. Biphasic electrical field stimulation aids in tissue engineering of multicell-type cardiac organoids. Tissue Eng A **17,** 1465, 2011.

23. Zimmermann, W.-H., Schneiderbanger, K., Schubert, P., Didie, M., Munzel, F., Heubach, J.F., Kostin, S., Neuhuber, W.L., and Eschenhagen, T. Tissue engineering of a differentiated cardiac muscle construct. Circ Res **90,** 223, 2002.

24. Fink, C., Ergün, S., Kralisch, D., Remmers, U., Weil, J., and Eschenhagen, T. Chronic stretch of engineered heart tissue induces hypertrophy and functional improvement. FASEB J **14,** 669, 2000.

25. Narmoneva, D.A., Vukmirovic, R., Davis, M.E., Kamm, R.D., and Lee, R.T. Endothelial cells promote cardiac myocyte survival and spatial reorganization: implications for cardiac regeneration. Circulation **110,** 962, 2004.

26. Radisic, M., Park, H., Martens, T.P., Salazar-Lazaro, J.E., Geng, W., Wang, Y., Langer, R., Freed, L.E., and Vunjak-Novakovic, G. Pre-treatment of synthetic elastomeric scaffolds by cardiac fibroblasts improves engineered heart tissue. J Biomed Mater Res A **86,** 713, 2008.

27. Legant, W.R., Pathak, A., Yang, M.T., Deshpande, V.S., McMeeking, R.M., and Chen, C.S. Microfabricated tissue gauges to measure and manipulate forces from 3D microtissues. Proc Natl Acad Sci U S A **106,** 10097, 2009.

28. Radisic, M., Euloth, M., Yang, L., Langer, R., Freed, L.E., and Vunjak-Novakovic, G. High-density seeding of myocyte cells for cardiac tissue engineering. Biotechnol Bioeng **82,** 403, 2003.

29. Tan, J.L., Tien, J., Pirone, D.M., Gray, D.S., Bhadriraju, K., and Chen, C.S. Cells lying on a bed of microneedles: an approach to isolate mechanical force. Proc Natl Acad Sci U S A **100,** 1484, 2003.

30. Klotzsch, E., Smith, M.L., Kubow, K.E., Muntwyler, S., Little, W.C., Beyeler, F., Gourdon, D., Nelson, B.J., and Vogel, V. Fibronectin forms the most extensible biological fibers displaying switchable force-exposed cryptic binding sites. Proc Natl Acad Sci U S A **106,** 18267, 2009.

31. Sage, D., Neumann, F.R., Hediger, F., Gasser, S.M., and Unser, M. Automatic tracking of individual fluorescence particles: application to the study of chromosome dynamics. IEEE Trans Image Process **14,** 1372, 2005.

32. Smotherman, W.P., Robinson, S.R., Ronca, A.E., Alberts, J.R., and Hepper, P.G. Heart rate response of the rat fetus and neonate to a chemosensory stimulus. Physiol Behav **50,** 47, 1991.

33. Zimmermann, W.H., Fink, C., Kralisch, D., Remmers, U., Weil, J., and Eschenhagen, T. Three-dimensional engineered heart tissue from neonatal rat cardiac myocytes. Biotechnol Bioeng **68,** 106, 2000.

34. Naito, H., Melnychenko, I., Didie, M., Schneiderbanger, K., Schubert, P., Rosenkranz, S., Eschenhagen, T., and Zimmermann, W.-H. Optimizing engineered heart tissue for therapeutic applications as surrogate heart muscle. Circulation **114(1 Suppl),** 172, 2006.

35. Hasenfuss, G., Mulieri, L., Blanchard, E., Holubarsch, C., Leavitt, B., Ittleman, F., and Alpert, N. Energetics of isometric force development in control and volume- overload human myocardium. Comparison with animal species. Circ Res **68,** 836, 1991.

36. Lorenzen-Schmidt, I., Schmid-Schönbein, G., Giles, W., McCulloch, A., Chien, S., and Omens, J. Chronotropic re-

sponse of cultured neonatal rat ventricular myocytes to short-term fluid shear. Cell Biochem Biophys **46,** 113, 2006.

37. Schubert, B., Vandongen, A.M., Kirsch, G.E., and Brown, A.M. Inhibition of cardiac Na + currents by isoproterenol. Am J Physiol Heart Circ Physiol **258(4 Pt 2),** H977, 1990.

38. Akera, T., Larsen, F.S., and Brody, T.M. Correlation of cardiac sodium- and potassium-activated adenosine triphosphatase activity with ouabain-induced inotropic stimulation. J Pharmacol Exp Ther **173,** 145, 1970.

39. Gadsby, D.C., Kimura, J., and Noma, A. Voltage dependence of Na/K pump current in isolated heart cells. Nature **315,** 63, 1985.

40. McGarry, S.J. and Williams, A.J. Digoxin activates sarcoplasmic reticulum Ca(2 + )-release channels: a possible role in cardiac inotropy. Br J Pharmacol **108,** 1043, 1993.

41. Ruch, S.R., Nishio, M., and Wasserstrom, J.A. Effect of cardiac glycosides on action potential characteristics and contractility in cat ventricular myocytes: role of calcium overload. J Pharmacol Exp Ther **307,** 419, 2003.

42. Shapira-Schweitzer, K., and Seliktar, D. Matrix stiffness affects spontaneous contraction of cardiomyocytes cultured within a PEGylated fibrinogen biomaterial. Acta Biomater **3,** 33, 2007.

43. Samuel, J.L., and Vandenburgh, H.H. Mechanically induced orientation of adult rat cardiac myocytes *in vitro*. In Vitro Cell Dev Biol **26,** 905, 1990.

44. Eschenhagen, T., Fink, C., Remmers, U., Scholz, H., Wattchow, J., Weil, J., Zimmermann, W., Dohmen, H., Schafer, H., Bishopric, N., Wakatsuki, T., and Elson, E. Three-dimensional reconstitution of embryonic cardiomyocytes in a collagen matrix: a new heart muscle model system. FASEB J **11,** 683, 1997.

45. Berry, M.F., Engler, A.J., Woo, Y.J., Pirolli, T.J., Bish, L.T., Jayasankar, V., Morine, K.J., Gardner, T.J., Discher, D.E., and Sweeney, H.L. Mesenchymal stem cell injection after myo-cardial infarction improves myocardial compliance. Am J Physiol Heart Circ Physiol **290,** H2196, 2006.

46. Engler, A.J., Carag-Krieger, C., Johnson, C.P., Raab, M., Tang, H.-Y., Speicher, D.W., Sanger, J.W., Sanger, J.M., and Discher, D.E. Embryonic cardiomyocytes beat best on a matrix with heart-like elasticity: scar-like rigidity inhibits beating. J Cell Sci **121,** 3794, 2008.

47. Young, J.L., and Engler, A.J. Hydrogels with time-dependent material properties enhance cardiomyocyte differentiation *in vitro*. Biomaterials **32,** 1002, 2011.

48. Leone, M., Albanèse, J., and Martin, C. Positive inotropic stimulation. Curr Opin Crit Care **8,** 395, 2002.

49. Tang, L., Gao, W., and Taylor, P.B. Force-frequency response in isoproterenol-induced hypertrophied rat heart. Eur J Pharmacol **318,** 349, 1996.

50. Schouten, V.J.A., and ter Keurs, H.E.D.J. Role of ica and Na + Ca2 + exchange in the force-frequency relationship of rat heart muscle. J Mol Cell Cardiol **23,** 1039, 1991.

51. Borzak, S., Murphy, S., and Marsh, J.D. Mechanisms of rate staircase in rat ventricular cells. Am J Physiol Heart Circ Physiol **260(3 Pt 2),** H884, 1991.

Address correspondence to:
*Christopher S. Chen, M.D., Ph.D.*
*Department of Bioengineering*
*University of Pennsylvania*
*220 S. 33rd St.*
*Skirkanich Hall Ste 510*
*Philadelphia, PA 19104*

*E-mail:* chrischen@seas.upenn.edu